

# Revisiting gluon density from the BK equation with kinematical constraint and large $x$ terms

Krzysztof Kutak<sup>1</sup>, Wanchen Li<sup>\*2</sup>, Anna Stasto<sup>3</sup>, and Robert Straka<sup>4</sup>

<sup>1</sup>Institute of Nuclear Physics, Polish Academy of Sciences, ul. Radzikowskiego 152, 31-342, Kraków, Poland

<sup>2</sup>Department of Physics and Center for Field Theory and Particle Physics, Fudan University, Shanghai 200438, China

<sup>3</sup>Department of Physics, Penn State University, University Park, PA 16802, U.S.A.

<sup>4</sup>AGH University of Science and Technology, Krakow, Poland

March 18, 2025

## Abstract

We perform analysis of the small  $x$  non-linear evolution equation formulated in momentum space supplemented by higher order terms. The equation is defined in wide range of transverse momentum and longitudinal momentum fraction extending previous studies performed in [1, 2]. The linear part of the equation is motivated by the renormalization group improved small  $x$  approach which accounts for resummation of higher orders, and includes collinear splitting function and kinematical constraint. The solution to the equation is then used to perform the fit to Deep Inelastic Scattering reduced cross section data.

## 1 Introduction

Present day high energy accelerators, like Large Hadron Collider (LHC) allow for the exploration of the new kinematic regime in particle interactions. Tests of the Standard Model are thus possible with unprecedented accuracy in the region where the total center-of-mass energy is much higher than the masses of the incoming hadrons. For the precise description of the processes in these collisions, a detailed knowledge of the partonic structure of the incoming hadrons is necessary. The information is encoded in the *parton distribution functions* (PDFs), which in the usual collinear factorization framework are obtained from the solution to the Dokshitzer-Gribov-Lipatov-Altarelli-Parisi (DGLAP) equations [3, 4, 5, 6]. These equations allow for the evolution of *integrated* PDFs with some hard scale  $Q^2$  and resum the large logarithms  $\ln Q^2/Q_0^2$  where  $Q_0$  is some reference

---

<sup>\*</sup>wanchenli@fudan.edu.cn

scale. The splitting functions for DGLAP evolution are known up to NNLO [7, 8] and recent intense theoretical efforts aim push the accuracy beyond that level.

An alternative framework for the calculation of the processes in the high energy limit is given by the  $k_T$  or *high energy factorization* [9, 10], where the structure of the hadron is encoded in the *unintegrated* gluon distribution function. This is usually referred to as the high-energy limit or the Regge limit, with  $s \gg |t|, m^2$ , where  $s$  is the center-of-mass energy squared,  $t$  is the momentum transfer squared, and  $m$  typical masses of the produced particles. The corresponding evolution is governed by the Balitsky-Fadin-Kuraev-Lipatov (BFKL) evolution equation [11, 12, 13], which sums up the powers of logarithms  $\ln s/s_0$  where  $s_0$  is a reference scale.

For the case of the Deep Inelastic Scattering process (DIS) of scattering electrons off protons, the energy scale  $s_0$  is taken to be equal to the (negative) virtuality of the photon  $Q^2$ . Therefore the BFKL resums large logarithms of  $\ln 1/x$ , where  $x \simeq Q^2/W^2$  is the Bjorken  $x$  variable with  $W^2$  being the square of the photon-proton energy. The solution to the BFKL equation results in the power like growth of the gluon density at small  $x$  and thus of the corresponding cross sections. The BFKL evolution equation is known up to NLL [14, 15] accuracy in QCD, and up to NNLL level in N=4 sYM theory [16, 17, 18]. The LL solution gives the power-like growth of the gluon density with the decreasing  $x$  as  $x^{-\omega_P}$ , with the LL intercept  $\omega_P = 4 \ln 2 \frac{\alpha_s N_c}{\pi} \sim 0.5$ . The solution at LL leads to the growth of structure functions that is too steep for the experimental data at HERA, e.g. [19]. The NLL order corrections turned out to be large and negative leading to instabilities, and thus triggered the need for the resummation of the higher order terms in order to stabilize the results.

The major ingredients of the resummation we implement in this paper are the kinematical constraint, DGLAP splitting function and the running of the strong coupling. One of the first approaches, by Kwieciński-Martin-Staśto (KMS) [20], used the unified the BFKL and DGLAP evolution. In this work the unified system of equations for the unintegrated gluon density was constructed which was based on the BFKL evolution equation supplemented with the kinematical constraint and the non-singular DGLAP evolution terms. Coupled with the equation for quarks, this system was shown to produce the gluon distribution which could be fitted to the structure function data from HERA, with only two free parameters. It contained both  $Q^2$  and  $x$  evolutions on equal footing. Based on this system of unified equation, a resummation framework was developed by Ciafaloni-Colferai-Salam-Staśto (CCSS) in a series of works [21, 22, 23, 24, 25, 26]. In that approach the Kwieciński-Martin-Staśto (KMS) [20] formulation was supplemented by the NLL terms of the BFKL, with appropriate subtractions as well as the anti-collinear terms. Recently the CCSS resummation was applied to the structure functions at HERA, and good description of the data at small values of  $x$  was obtained [27].

In the region of very small  $x$ , there are additional effects that need to be taken into account. When the gluon density becomes very high, recombination of gluons, will start to play an important role, leading to the taming of the rapid growth. This is referred to as *parton saturation* [28, 29]. The effective theory which describes the limit of high energy and density QCD is the Color Glass Condensate (CGC) [30, 31, 32], with the corresponding Jalilian-Marian-Iancu-Weigert-Leonidov-Kovner (JIMWLK) evolution equations [33, 34,

35, 36, 37, 38]. An equivalent approach is based on the operator expansion at high energy, together with the corresponding Balitsky hierarchy equations [39, 40]. When the large color limit  $N_C$  is taken, this hierarchy allows for the decoupling of the nonlinear equation, the Balitsky-Kovchegov (BK) evolution equation [40, 41, 42] for the dipole scattering amplitude. It was later shown that the subleading- $N_C$  corrections is very small, resulting only 0.1% difference between the JIMWLK and BK simulations [43]. The BK equation contains the non-linear term responsible for the gluon recombination, and the solution can be characterized by the presence of the dynamically generated, energy dependent, saturation scale  $Q_s(x)$ , which divides the region between the dilute and dense regimes.

The BK equation is originally formulated for the dipole amplitude and thus it is written in the coordinate space [39, 41, 42]. Recently it has been generalized and solved at NLO accuracy [44, 45]. In papers [1, 46, 47] the BK evolution equation has been rederived in the momentum space, and in [48] this non-linear term was included in the KMS [20] formulation. The gluon density obtained by solving this equation was used to successfully describe the  $F_2$  structure function data and was used in numerous phenomenological applications [49, 50, 51, 52, 53]. One assumption of [20, 48] was that the solution was truncated by an infrared cutoff and extrapolated ‘by hand’ to lower transverse momentum  $k_T$ . On the other hand, it is customary to solve the BK evolution equation for large dipole sizes, when using its solutions to fit to the structure function data [48], where the non-perturbative contribution is usually taken automatically into account by integration over the large dipole sizes with the flat dipole cross section, see e.g. [54, 55, 56, 57]

In this paper we extend the Kutak-Sapeta (KS) approach of [48] and solve the non-linear BK equation in momentum space including running coupling, non-singular part of the DGLAP splitting function for both collinear and anti-collinear regions as well as kinematical constraint. The non-linear term regulates the behavior at very low transverse momenta, and therefore it allows for extending the solution to this region. Unlike other approaches for the resummed BK [58], this formulation in momentum space allows for the inclusion of the full DGLAP gluon splitting function in the evolution on an equal footing to the BFKL kernel. The initial condition is given by a form motivated by the momentum space Golec-Biernat, Wusthoff (GBW) model [59], and the fit is performed to the reduced cross section data from HERA [60], and consistent description is achieved. This formulation can be easily extended to include the full CCSS resummation for the linear term, as it has been done in [27], and also for the case of nuclei, by rescaling the radius parameter by  $A^{1/3}$  for the non-linear term. Considering the numerical aspects: we iteratively solve an integro-differential evolution equation eq. (1) for consecutive values of  $x$  starting from  $x = 1$ . Our numerical algorithm is implemented in CUDA C that enabled parallel evaluation of the equation eq. (1) with respect to  $k^2$ . Moreover, the converged part of solution for previous values of  $x$  is used in integration with respect to next value of  $x$ , parts of DGLAP integrals are precomputed and tabulated. Aforementioned optimizations allowed for a considerable speedup compared to a sequential code.

The structure of the paper is as follows: In section 2, we begin with the LL BK equation in momentum space and outline the higher-order resummation improvements implemented in the equation. Section 3 introduces the  $k_T$  factorization framework, which allows us to compute the structure functions. In section 4, we present our fits to the

HERA data and analyze the behavior of the resulting gluon density. Finally, we conclude in section 5.

## 2 LL BK in momentum space equation and resummations

### 2.1 LL BK equation in momentum space

The BK equation was originally derived in the coordinate space [40, 41, 42]. It can be reformulated in the momentum space [1, 61]. The equation for unintegrated gluon density  $\mathcal{F}(x, k^2)$  as a function of longitudinal momentum fraction  $x$  and transverse momentum  $k$  reads

$$\begin{aligned} \mathcal{F}(x, k^2) = & \mathcal{F}^{(0)}(x, k^2) + \\ & + \int_x^1 \frac{dz}{z} \int dk'^2 \bar{\alpha}_s(k^2, k'^2) \left[ \frac{\mathcal{F}(\frac{x}{z}, k'^2)}{|k^2 - k'^2|} - \frac{k^2}{k'^2} \frac{\mathcal{F}(\frac{x}{z}, k^2)}{|k^2 - k'^2|} + \frac{k^2}{k'^2} \frac{\mathcal{F}(\frac{x}{z}, k^2)}{\sqrt{k^4 + 4k'^4}} \right] + \\ & - \frac{2\pi^3}{N_c^2 R^2} \int_x^1 \frac{dz}{z} \left\{ \left[ \int_{k^2}^{\infty} \frac{dl^2}{l^2} \bar{\alpha}_s(k^2, l^2) \mathcal{F}(\frac{x}{z}, l^2) \right]^2 + \right. \\ & \left. + \mathcal{F}(\frac{x}{z}, k^2) \int_{k^2}^{\infty} \frac{dl^2}{l^2} \bar{\alpha}_s^2(k^2, l^2) \ln \left( \frac{l^2}{k^2} \right) \mathcal{F}(\frac{x}{z}, l^2) \right\} , \quad (1) \end{aligned}$$

where  $\mathcal{F}^{(0)}$  is starting distribution. The linear part of the equation (the second line) corresponds to the angular averaged BFKL kernel whose real part represents emission of gluons and virtual corresponding to the reggeization. The nonlinear part (the third and fourth lines) accounts for recombination of gluons and is given by triple Pomeron vertex, here angular averaged [46]. The strength of the nonlinear term is controlled by the effective radius of proton or nucleus  $R$ , which will be one of the fitting parameters. In the coordinate space based derivation, this parameter originates from the assumption that the target is a large, homogeneous disk of radius  $R$ . After performing a Fourier transform from coordinate space to momentum space, integrating over the impact parameter, and normalizing the resulting gluon density so that  $\int d^2b \mathcal{F}(x, k^2, b) = \mathcal{F}(x, k^2)$  the nonlinear term gains the  $1/R^2$  factor<sup>1</sup>. In the above the rescaled coupling constant is  $\bar{\alpha}_s(k^2, k'^2) = N_c \alpha_s(\max(k^2, k'^2)) / \pi$  with number of colors  $N_c = 3$ . In the LO the strong coupling is fixed in the high energy limit, it starts to run at NLO order. The NLL calculation [14, 15] suggests that the natural scale as the argument of the running coupling is the virtuality of the emitted gluon  $q^2 = (k - k')^2$  (see fig. 7), see also a discussion in [25]. Here we use a choice of  $\max(k'^2, k^2)$  which is numerically close to the above choice and also symmetric with respect to  $k^2, k'^2$ . In the present calculation we aim to solve eq. (1) down to very low transverse momenta. Therefore we need some form of regularization of the strong

---

<sup>1</sup>For more details see recent review [53].

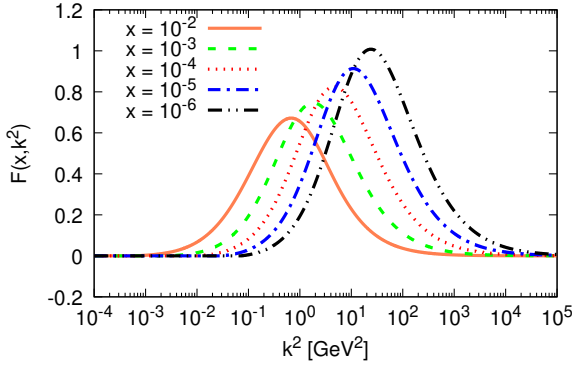


Figure 1: Solution of BK equation from eq. (1) as function of  $k^2$  for various values of  $x$ .

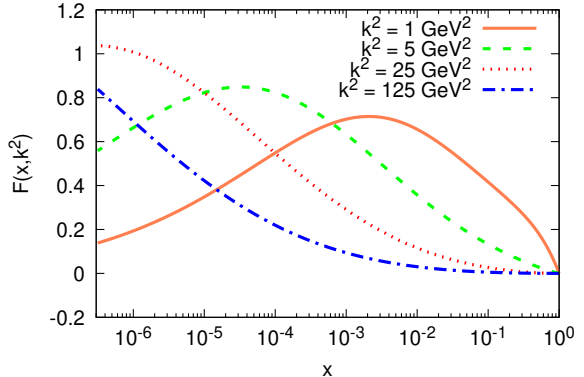


Figure 2: Solution of BK equation from eq. (1) as function of  $x$  for various values of  $k^2$ .

coupling. We shall take the parametrization [62, 63]

$$\alpha_s(k^2) = \frac{12\pi}{33 - 2N_f} F(k, k_{fr}, \Lambda_{QCD}) , \quad (2)$$

where

$$F(k, k_{fr}, \Lambda_{QCD}) = \left[ \log \left( \frac{k^2 + k_{fr}^2}{\Lambda_{QCD}^2} \right) \right]^{-1} - \frac{\Lambda_{QCD}^2}{k^2 + k_{fr}^2 - \Lambda_{QCD}^2} , \quad (3)$$

with number of flavors  $N_f = 4$  parameter  $k_{fr}^2 = 1.4 \text{ GeV}^2$  obtained by fitting the  $\alpha_s$  from [64]. The formula follows from studies of analyticity properties of QCD coupling constant and was recently used in successful description of  $F_2$  at small values of  $Q^2$  [65]. Furthermore it gives smooth extrapolation of the strong coupling to small transverse momenta.

In the following we shall illustrate basic properties and behavior of the solution to eq. (1) at lowest order, including only the running coupling.

In figs. 1 and 2 we present the solution of the eq. (1) using the initial condition given by input motivated by the GBW model

$$\mathcal{F}^{(0)}(x, k^2) = (1 - x)^\alpha k^2 e^{-k^2/Q_s^2} . \quad (4)$$

In the above we set the saturation scale  $Q_s^2 = 1 \text{ GeV}^2$  and  $\alpha = 1$ , where we take  $R^2 \approx 8.0 \text{ GeV}^{-2}$  in eq. (1), which is the result of the our later reduced cross section fit in section 4. The factor  $(1 - x)^\alpha$  proposed in [66] regulates the behavior of the starting distribution at  $x = 1$ . This is necessary especially in the case when DGLAP terms are included, as studied later in this section. In fig. 1 the solution is shown as a function of the transverse momentum for several values of  $x$ . As  $x$  becomes lower, the typical value of transverse momentum characterized by the saturation scale becomes larger and larger. In fig. 2,  $x$  dependence is illustrated and we observe that, for small transverse momentum, the gluon density has a valence-like behavior at small  $x$ . As  $k^2$  becomes larger than the saturation scale, the falling part of gluon density happens at lower  $x$ .

## 2.2 Higher order improvements to the BK evolution

The equation discussed above is LL in  $\alpha_s \ln 1/x$  and subject to large corrections [14, 15, 67] at higher orders. Below we will use the prescription developed by [23, 25]. The equation with resummed higher order corrections assumes the schematic form

$$\mathcal{F}(x, k^2) = \mathcal{F}^{(0)}(x, k^2) + \mathcal{K}_{res} \otimes \mathcal{F}(x, k^2) - \mathcal{V} \otimes \mathcal{F}^2(x, k^2) , \quad (5)$$

with

$$\mathcal{K}_{res} \otimes \mathcal{F} \equiv \mathcal{K}_0^{kc}(z; k, k') \stackrel{z, k'}{\otimes} \mathcal{F}\left(\frac{x}{z}, k'\right) + \mathcal{K}_0^{\text{coll}}(z; k, k') \stackrel{z, k'}{\otimes} \mathcal{F}\left(\frac{x}{z}, k'\right) . \quad (6)$$

The first term in Eq. (6) is

$$\begin{aligned} \mathcal{K}_0^{kc}(z; k, k') \stackrel{z, k'}{\otimes} \mathcal{F}\left(\frac{x}{z}, k'\right) = \\ \int_x^1 \frac{dz}{z} \int dk'^2 \bar{\alpha}_s(k^2, k'^2) \left[ \frac{\mathcal{F}\left(\frac{x}{z}, k'^2\right)}{|k^2 - k'^2|} \Theta\left(\frac{k^2}{z} - k'^2\right) - \frac{k^2}{k'^2} \frac{\mathcal{F}\left(\frac{x}{z}, k^2\right)}{|k^2 - k'^2|} + \frac{k^2}{k'^2} \frac{\mathcal{F}\left(\frac{x}{z}, k^2\right)}{\sqrt{k^4 + 4k'^4}} \right] \end{aligned} \quad (7)$$

The kinematical (or consistency) constraint  $\Theta\left(\frac{k^2}{z} - k'^2\right)$  term is implemented onto the real emissions only. It is here asymmetric, which corresponds to the asymmetric scale choice suitable for the DIS problem we are considering. It is implemented as

$$k'^2 \leq \frac{k^2}{z} . \quad (8)$$

In fig. 3 we show solution of BK equation with kinematical constraint. We see that the normalization of gluon density changed almost by factor 2 as compared to the running coupling BK gluon in figs. 1 and 2. Growth with decreasing  $x$  is slowed down and the valence like behavior is observed for low values of  $k^2$  only<sup>2</sup>.

The second contribution in (6) is

$$\begin{aligned} \mathcal{K}_0^{\text{coll}}(z; k, k') \stackrel{z, k'}{\otimes} \mathcal{F}\left(\frac{x}{z}, k'\right) = \int_x^1 \frac{dz}{z} \int_0^{k^2} \frac{dk'^2}{k^2} \bar{\alpha}_s(k^2) z \tilde{P}_{gg}(z) \mathcal{F}\left(\frac{x}{z}, k'\right) \\ + \int_x^1 \frac{dz}{z} \int_{k^2}^{k^2/z} \frac{dk'^2}{k'^2} \bar{\alpha}_s(k'^2) z \frac{k'^2}{k^2} \tilde{P}_{gg}\left(z \frac{k'^2}{k^2}\right) \mathcal{F}\left(\frac{x}{z}, k'\right) . \end{aligned} \quad (9)$$

It is the sum of the collinear and anticollinear parts with the non-singular part of the splitting function

$$\tilde{P}_{gg}^{(0)} = P_{gg}^{(0)} - \frac{1}{z} , \quad (10)$$

where the  $P_{gg}^{(0)}$  is the DGLAP gluon-gluon splitting function in LO given by

$$P_{gg}^{(0)} = \frac{1-z}{z} + z(1-z) + \frac{z}{(1-z)_+} + \frac{1}{2C_A} \delta(1-z) \frac{11C_A - 4N_f T_r}{6} . \quad (11)$$

<sup>2</sup>For work addressing accounting for kinematical constraint in the coordinate space BK equation see [68] pointing out relevance of kinematical constraint in the context of jet physics and NLO corrections see [69].

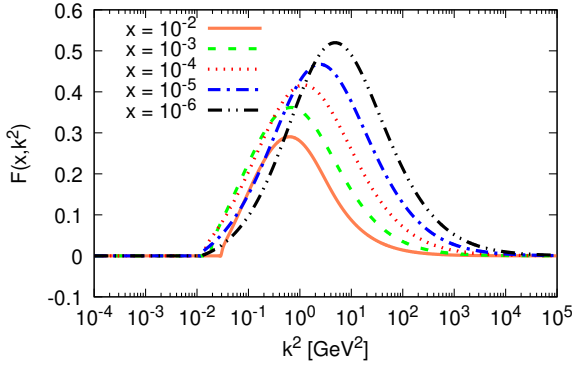


Figure 3: Solution of BK equation supplemented with kinematical constraint as a function of  $k^2$  for various values of  $x$ .

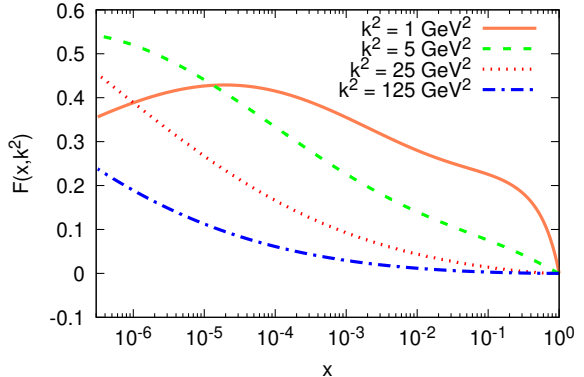


Figure 4: Solution of BK equation supplemented with kinematical constraint as a function of  $x$  for various values of  $k^2$ .

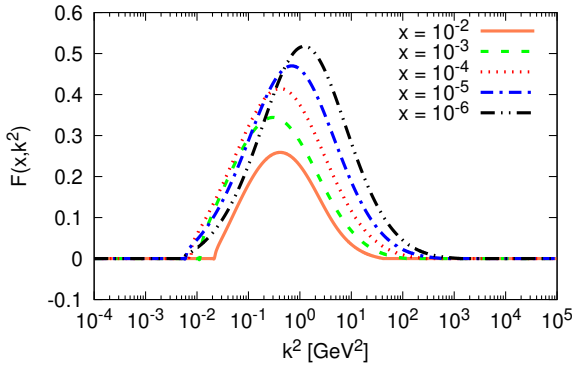


Figure 5: Solution of BK equation supplemented with kinematical constraint and DGLAP as a function of  $k^2$  for various values of  $x$ .

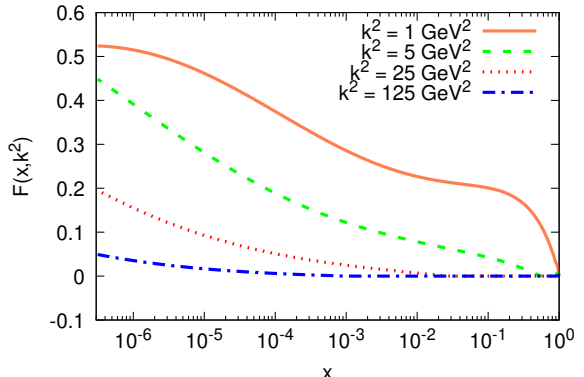


Figure 6: Solution of BK equation supplemented with kinematical constraint and DGLAP as a function of  $x$  for various values of  $k^2$ .

Here  $C_A = 3$ ,  $T_r = 1/2$  and  $N_f$  is number of quark flavors. We stress that one of the big advantages of the formulation of the evolution in the momentum space is the ability to include the full DGLAP terms. In fig. 5 we present the solution of the BK supplemented with DGLAP correction and kinematical constraint. Compared to the scenario that accounts for running coupling and the kinematical constraint, the inclusion of DGLAP further suppresses the unintegrated gluon density, leading to a flatter  $x$ -spectrum.

### 3 Structure function in the $k_T$ factorization

The DIS structure functions  $F_2$  in the small  $x$  region can be expressed as a convolution of the off-shell photon-gluon partonic cross section with the unintegrated gluon density. The longitudinal structure function  $F_L$ , which is a necessary contribution to compute the reduced cross section, can be calculated in a same fashion, see e.g. [70]. This scheme,

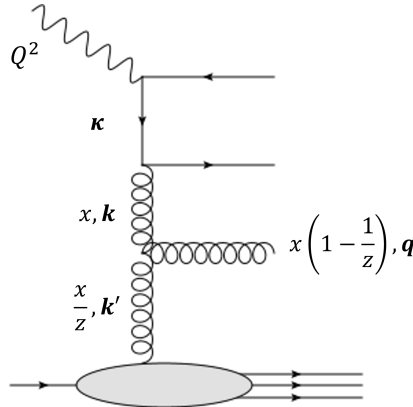


Figure 7: DIS diagram in the high energy factorization, where the transverse momentum of the emitting gluon  $\mathbf{q} = \mathbf{k}' - \mathbf{k}$ .

known as  $k_T$  factorization [9, 10, 71], is illustrated schematically in fig. 7.

The perturbative contribution to the structure function  $F_2$  from the  $k_T$  factorization is given by

$$F_2(x, Q^2) = \sum_q e_q^2 S_q(x, Q^2), \quad (12)$$

where the sum is over the quark flavors and  $S_q(x, Q^2)$  can be factorized into the following form

$$S_q(x, Q^2) = \int_x^1 \frac{dz}{z} \int dk^2 S_{\text{box}}^q(z, m_q^2, k^2, Q^2) \mathcal{F}\left(\frac{x}{z}, k^2\right). \quad (13)$$

Here,  $S_{\text{box}}^q$  is the off-shell photon-gluon partonic cross section (*box* named after the calculation of the amplitude of fig. 7 with its conjugate).

The explicit expression of eq. (13) after the Sudakov decomposition is given by [72, 20]

$$S_q(x, Q^2) = \frac{Q^2}{4\pi^2} \int_{k_{\min}^2}^{\infty} \frac{dk^2}{k^2} \int_0^1 d\beta \int d\kappa' \alpha_s(\mu^2) \left\{ \left[ \beta^2 + (1 - \beta^2) \right] \left( \frac{\kappa}{D_{1q}} - \frac{\kappa - \mathbf{k}}{D_{2q}} \right)^2 + \left[ m_q^2 + 4Q^2\beta^2(1 - \beta)^2 \right] \left( \frac{1}{D_{1q}} - \frac{1}{D_{2q}} \right)^2 \right\} \mathcal{F}\left(\frac{x}{z}, k^2\right) \Theta\left(1 - \frac{x}{z}\right), \quad (14)$$

where  $\kappa$  and  $\mathbf{k}$  are quark and gluon transverse momenta respectively, and  $\beta$  is the longitudinal momentum fraction of the photon carried by the quark variable defined in the of the quark momentum (see Sudakov decomposition in [72]). Instead of integrating on  $\kappa$ , it turns out to be convenient to work with the shifted quark transverse momentum  $\kappa' = \kappa - (1 - \beta)\mathbf{k}$ . Masses of the quarks are denoted by  $m_q$ .

The energy denominators are defined as

$$D_{1q} = \kappa^2 + \beta(1 - \beta)Q^2 + m_q^2, \quad (15)$$

$$D_{2q} = (\kappa - \mathbf{k})^2 + \beta(1 - \beta)Q^2 + m_q^2. \quad (16)$$

In addition, the argument of the unintegrated gluon density from the resummed BK equation is  $x/z$ , where

$$z = \left[ 1 + \frac{\kappa'^2 + m_q^2}{\beta(1-\beta)Q^2} + \frac{k^2}{Q^2} \right]^{-1}. \quad (17)$$

This prescription above arises from a rigorous treatment of the photon-gluon fusion process, incorporating its exact kinematic [72]. In the  $k_T$  factorization framework, such a precise kinematic description elevates the photon impact factor beyond LL approximations [73, 74] yielding significant phenomenological consequences, as demonstrated in [70]. Notably, recent advances have enabled collinear resummation to the photon impact factor [75], which retain consistency with the exact kinematic formulation in the collinear limit<sup>3</sup>.

We take the argument of the strong coupling  $\alpha_s$  to be  $\mu^2 = k^2 + \kappa'^2 + m_q^2$ , while the masses of quarks are  $m_u = m_d = m_s = 0$  and  $m_c = 1.4$  GeV.

In principle, the  $k_T$  factorization approach requires integrating over the transverse momentum  $\kappa$  down to zero in eq. (14), which extends into the non-perturbative region. Meanwhile, although the non-linear BK evolution allows the unintegrated gluon density  $\mathcal{F}(x, k^2)$  to be evolved into the low gluon transverse momentum  $k$  region, it does not alter the infrared behavior of the quark transverse momentum  $\kappa$ . Therefore following [20], we include a separate non-perturbative contribution. This follows from the well known fact, the structure function  $F_2$  receives large soft contribution. As proposed in [77], this soft or non-perturbative contribution has been simply parametrized as the constant background term in addition to the perturbative contribution. In the approaches within the dipole model, the non-perturbative contribution corresponds to integration over the large dipole sizes with the flat dipole cross section, see for example discussion in [54, 55]. For small values of  $\kappa$ , this non-perturbative region corresponds to the so-called *soft Pomeron exchange* contribution [78], which can be parametrized phenomenologically as

$$S^{(a)} = S_u^{\mathbb{P}} + S_d^{\mathbb{P}} + S_s^{\mathbb{P}}, \quad (18)$$

for light quarks and

$$S_u^{\mathbb{P}} = S_d^{\mathbb{P}} = 2S_s^{\mathbb{P}} = C_{\mathbb{P}} x^{-\lambda} (1-x)^8, \quad (19)$$

where coefficient  $C_{\mathbb{P}}$  is a free parameter independent of  $Q^2$  and  $\lambda$  is the soft Pomeron power to be fitted from experimental data. We assume that the charm contribution is generated purely perturbatively, and therefore there is no soft Pomeron contribution corresponding to it, i.e.  $S_c^{\mathbb{P}} = 0$ .

By noting the perturbative contribution to the structure function in eq. (14) as  $S^{\text{pert}}$ , the total structure functions  $F_2$  is therefore simply

$$F_2 = \sum_q e_q^2 (S_q^{\mathbb{P}} + S^{\text{pert}}). \quad (20)$$

---

<sup>3</sup>For recent work on evaluation of  $F_2$  in coordinate space at NLO accuracy see [76].

## 4 Fit results

In this section, we present the fit to HERA data [60] and the corresponding unintegrated gluon density, i.e. the solution of eq. (5). We choose the following initial condition inspired by the GBW model,

$$\mathcal{F}^{(0)}(x, k) = A \alpha_s(k^2) (1-x)^\alpha x^\beta (k^2)^\gamma e^{-B^2 k^2}. \quad (21)$$

The parameters are fitted to the reduced cross section  $\sigma_r$ , which is given by the combination of the two structure functions  $F_2$  and  $F_L$

$$\sigma_r(y, x, Q^2) = F_2(x, Q^2) - \frac{y^2}{1 + (1-y)^2} F_L(x, Q^2). \quad (22)$$

Here, the inelasticity  $y = Q^2/(sx)$  and  $\sqrt{s}$  is the electron-proton collision energy. We set the flavor number  $N_f = 4$ .

In fig. 8 we present our fit compared with HERA data. By selecting all low  $x$  data ( $x < 0.013$ ), we fit a total of 239 data points. We propose two fit scenarios: one with fixed  $\Lambda_{\text{QCD}} = 0.289$  GeV, matching the choice in [27], and the other where  $\Lambda_{\text{QCD}}$  is treated as a free fit parameter. Both fits provide a consistent description of the HERA data, and the obtained fit parameter values are summarized in table 1.

	$\alpha$	$\beta$	$A$	$B^2$	$\gamma$	$C_{\mathbb{P}}$	$\lambda$	$R^2$	$\Lambda_{\text{QCD}}$
$\chi^2/\text{dof} = 1.6$	0.80662	-0.42651	0.74038	0.64239	1.09987	0.6163	-0.02361	7.85408	0.499
$\chi^2/\text{dof} = 2.0$	0.67356	-0.41625	0.65917	0.47992	1.05338	0.572	-0.00223	8.00833	fixed

Table 1:  $\chi^2$  and fit parameters in the fitted and fixed  $\Lambda_{\text{QCD}}$  scenarios respectively.

The solutions with fitted  $\Lambda_{\text{QCD}}$  (solid curve) and fixed  $\Lambda_{\text{QCD}}$  (dashed curve) are presented in fig. 9 and fig. 10. The cusp appearing for lowest values of  $x$  around  $k^2 \sim 1$  GeV $^2$  in fig. 9 is due to the cut we enforced in the solver to prevent slightly negative values of the unintegrated gluon density. In fig. 9, both transverse momentum spectrum of the fitted and fixed  $\Lambda_{\text{QCD}}$  fit resembles very much the characteristic scaling behavior of the saturation scales, i.e. as  $x$  becomes smaller the saturation scale grows and gluon momenta are pushed toward perturbative region.

In fig. 10, we observe that the gluon densities in two scenarios are generally close, except for the curves with  $k^2 = 1$  GeV $^2$ , where our negativity limiter has a more significant impact. We comment that the underlying negative contributions stem from the interplay of negative nonlinear term in the BK equation and the collinear resummations in the linear part of the equation. Notably, our current resummed BK equation incorporates the kinematical constraint only in the linear term, making negative values more likely to appear. A possible improvement would be to introduce the kinematical constraint also in the nonlinear term. At present, such a constraint on the nonlinear term has been implemented in the BK equation only within the dipole model and in position space [68, 79, 80]. We plan to further investigate its effects within our formalism in future work.

In fig. 11, fig. 12 we show comparison of obtained gluon density to KSlinear, KSnonlinear [48] and Li-Stasto(LS)[27]. The main difference between our gluon density and

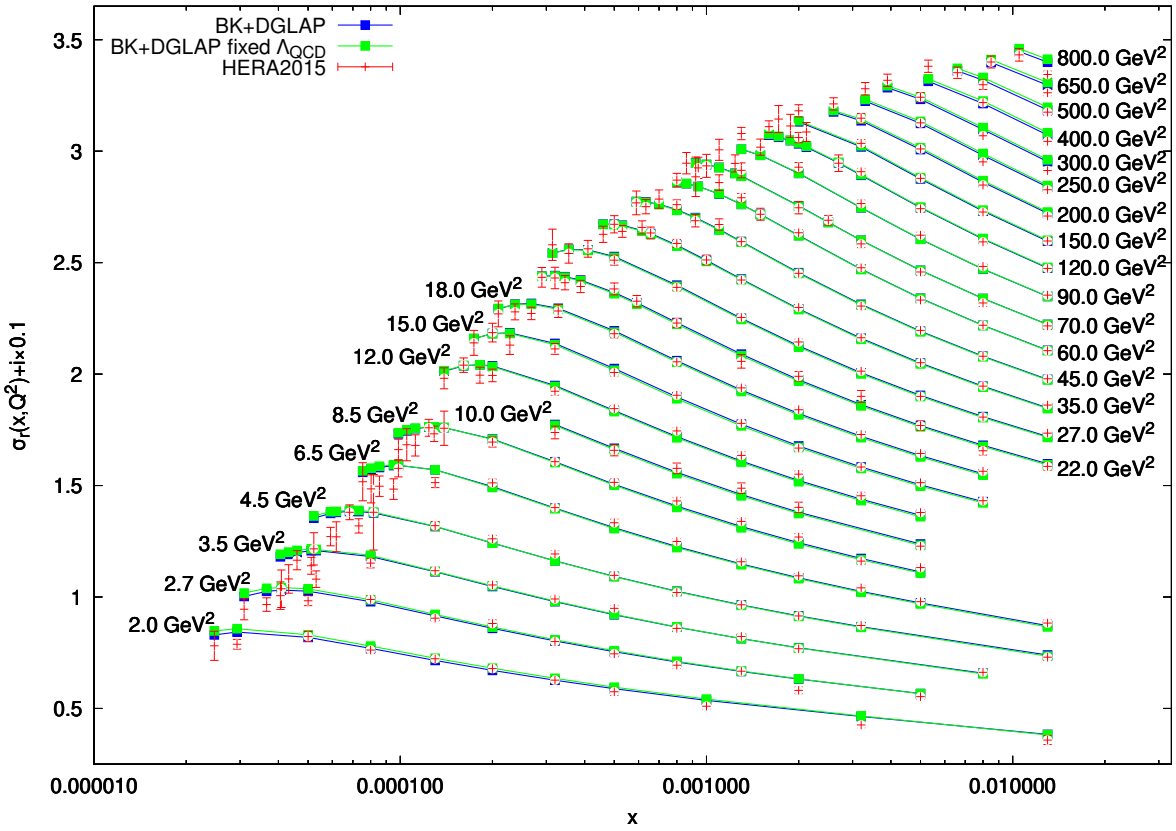


Figure 8: Comparison between our reduced cross section fit with the HERA data. Each curve is separated with an additional offset 0.1 to better present a wider  $Q^2$  spectrum. The blue curve is for fitted  $\Lambda_{\text{QCD}}$  and green curve for fixed  $\Lambda_{\text{QCD}} = 0.289 \text{ GeV}$ .

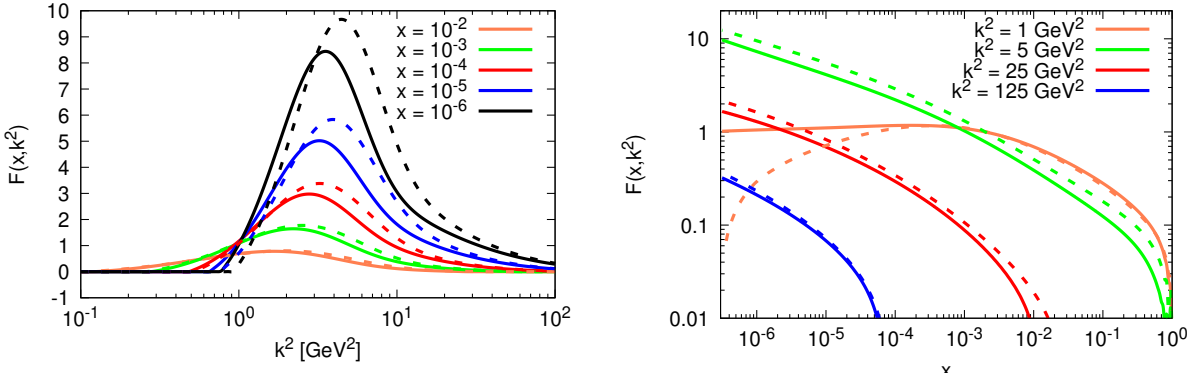


Figure 9: Plots of fitted unintegrated gluon density as a function of  $k^2$  for various values of  $x$ . Solid and dashed curves denote fitted and fixed  $\Lambda_{\text{QCD}}$ .

Figure 10: Plots of fitted unintegrated gluon density as a function of  $x$  for various values of  $k^2$ . Solid and dashed curves denote fitted and fixed  $\Lambda_{\text{QCD}}$ .

the other distributions is that we account for perturbative evolution down to low  $k$  of gluon. In practice, we set the lower bound  $k_{\min}^2 = 10^{-6} \text{ GeV}^2$ . This is possible because

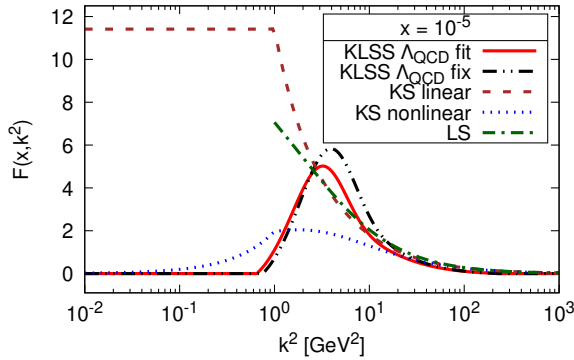


Figure 11: Plots of fitted unintegrated gluon density (with fixed and fitted  $\Lambda_{\text{QCD}}$ ) as a function of  $k^2$  for  $x = 10^{-5}$  compared to KS linear, KS nonlinear and LS linear gluon densities.

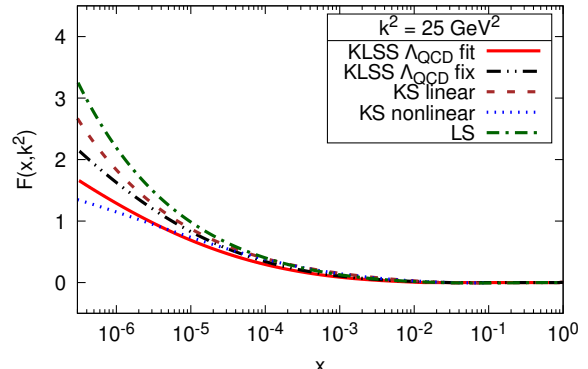


Figure 12: Plots of the unintegrated gluon densities (with fixed and fitted  $\Lambda_{\text{QCD}}$ ) as a function of  $x$  for  $k^2 = 25 \text{ GeV}^2$  compared to KS linear, KS nonlinear and LS linear gluon densities.

the nonlinear BK term regulates the infrared behavior of the linear BFKL evolution. The consequence of that is that the integral with the box eq. (13) can be evaluated directly with eq. (14) without splitting it to perturbative and non-perturbative parts, where a separated collinear approximation is typically applied [27, 48, 81]. This leads to larger gluon density as compared to other gluon densities. We note that in the KS nonlinear, the method of solving the equation did not allow to go to transverse momentum smaller than  $1 \text{ GeV}^2$  and extrapolation was used in this region. The  $F_2$  was calculated in similar manner as in KS linear and LS.

## 5 Conclusions

In this paper we investigated the momentum space BK equation with running coupling, kinematical constraint and DGLAP terms both in collinear and anticollinear limit. We first studied solutions for particular cases: including only the effects of kinematical constraint and kinematical constraint together with DGLAP terms. We demonstrated that each of these contributions have substantial impact on resulting solution and as it changes overall change normalisation and shape of gluon density. This is in agreement with previous findings by [2]. However the present formulation allows for extending the solution to small transverse momentum scales. This procedure impacts the resulting gluon density in such way that in non saturated region it is larger than the KS [48] gluon density while it is smaller in the saturated region. This may have important phenomenological consequences e.g for jet physics [82, 83, 50, 84, 85, 48, 53].

We used the obtained dipole gluon density together with impact factor with exact kinematics to calculate DIS reduced cross section. The form of the starting distribution was motivated by the Golec-Biernat-Wuesthoff model, but included additional modifications and parameters as required by the fit. Finally we would like to add that although there is some modeling involved the equation that we proposed is in line of the CCSS resummation, in order to complete it one needs to account for remaining NLO contribu-

tions as it has been done in the linear case in [27]. We leave the study of equation with these modifications for the future research.

## Acknowledgments

KK thanks Hannes Jung for informative discussions. KK acknowledges support from grant No. 2019/33/B/ST2/02588 (2020-23). AMS is supported by the U.S. Department of Energy grant No. DE-SC-0002145 and within the framework of the of the Saturated Glue (SURGE) Topical Theory Collaboration. WL is supported by the National Science Foundations of China under Grant No. 12275052, No. 12147101. RS is supported by the AGH University of Science and Technology, Faculty of Metals Engineering and Industrial Computer Science, Work no. 16.16.110.663.

## References

- [1] K. Kutak and J. Kwiecinski, *Screening effects in the ultrahigh-energy neutrino interactions*, *Eur. Phys. J. C* **29** (2003) 521, [[hep-ph/0303209](#)].
- [2] K. Kutak and A. M. Stasto, *Unintegrated gluon distribution from modified BK equation*, *Eur. Phys. J. C* **41** (2005) 343–351, [[hep-ph/0408117](#)].
- [3] Y. L. Dokshitzer, *Calculation of the Structure Functions for Deep Inelastic Scattering and  $e^+e^-$  Annihilation by Perturbation Theory in Quantum Chromodynamics.*, *Sov. Phys. JETP* **46** (1977) 641–653.
- [4] V. N. Gribov and L. N. Lipatov, *Deep inelastic ep scattering in perturbation theory*, *Sov. J. Nucl. Phys.* **15** (1972) 438–450.
- [5] V. N. Gribov and L. N. Lipatov,  *$e^+e^-$  pair annihilation and deep inelastic ep scattering in perturbation theory*, *Sov. J. Nucl. Phys.* **15** (1972) 675–684.
- [6] G. Altarelli and G. Parisi, *Asymptotic Freedom in Parton Language*, *Nucl. Phys.* **B126** (1977) 298–318.
- [7] A. Vogt, S. Moch and J. A. M. Vermaasen, *The Three-loop splitting functions in QCD: The Singlet case*, *Nucl. Phys. B* **691** (2004) 129–181, [[hep-ph/0404111](#)].
- [8] S. Moch, J. A. M. Vermaasen and A. Vogt, *The Three loop splitting functions in QCD: The Nonsinglet case*, *Nucl. Phys. B* **688** (2004) 101–134, [[hep-ph/0403192](#)].
- [9] S. Catani, M. Ciafaloni and F. Hautmann, *High-energy factorization and small x heavy flavor production*, *Nucl. Phys. B* **366** (1991) 135–188.
- [10] S. Catani, M. Ciafaloni and F. Hautmann, *GLUON CONTRIBUTIONS TO SMALL x HEAVY FLAVOR PRODUCTION*, *Phys. Lett. B* **242** (1990) 97–102.

- [11] I. I. Balitsky and L. N. Lipatov, *The Pomeranchuk Singularity in Quantum Chromodynamics*, Sov. J. Nucl. Phys. **28** (1978) 822–829.
- [12] E. A. Kuraev, L. N. Lipatov and R. S. Fadin, *The Pomeranchuk Singularity in Nonabelian Gauge Theories*, Sov. Phys. JETP **45** (1977) 199–204.
- [13] L. N. Lipatov, *The Bare Pomeron in Quantum Chromodynamics*, Sov. Phys. JETP **63** (1986) 904–912.
- [14] V. S. Fadin and L. N. Lipatov, *BFKL pomeron in the next-to-leading approximation*, Phys. Lett. B **429** (1998) 127–134, [[hep-ph/9802290](#)].
- [15] M. Ciafaloni and G. Camici, *Energy scale(s) and next-to-leading BFKL equation*, Phys. Lett. B **430** (1998) 349–354, [[hep-ph/9803389](#)].
- [16] V. N. Velizhanin, *BFKL pomeron in the next-to-next-to-leading approximation in the planar  $N=4$  SYM theory*, [1508.02857](#).
- [17] N. Gromov, F. Levkovich-Maslyuk and G. Sizov, *Pomeron Eigenvalue at Three Loops in  $\mathcal{N} = 4$  Supersymmetric Yang-Mills Theory*, Phys. Rev. Lett. **115** (2015) 251601, [[1507.04010](#)].
- [18] S. Caron-Huot and M. Herranen, *High-energy evolution to three loops*, Journal of High Energy Physics **2018** (2018) 58.
- [19] I. Bojak and M. Ernst, *Small  $x$  resummations confronted with  $F_2(x, Q^2)$  data*, Phys. Lett. B **397** (1997) 296–304, [[hep-ph/9609378](#)].
- [20] J. Kwiecinski, A. D. Martin and A. M. Stasto, *A Unified BFKL and GLAP description of  $F_2$  data*, Phys. Rev. **D56** (1997) 3991–4006, [[hep-ph/9703445](#)].
- [21] M. Ciafaloni, D. Colferai and G. P. Salam, *A collinear model for small  $x$  physics*, JHEP **10** (1999) 017, [[hep-ph/9907409](#)].
- [22] M. Ciafaloni, D. Colferai and G. P. Salam, *Renormalization group improved small  $x$  equation*, Phys. Rev. **D60** (1999) 114036, [[hep-ph/9905566](#)].
- [23] M. Ciafaloni, D. Colferai, D. Colferai, G. P. Salam and A. M. Stasto, *Extending QCD perturbation theory to higher energies*, Phys. Lett. B **576** (2003) 143–151, [[hep-ph/0305254](#)].
- [24] M. Ciafaloni, D. Colferai, G. P. Salam and A. M. Stasto, *The Gluon splitting function at moderately small  $x$* , Phys. Lett. **B587** (2004) 87–94, [[hep-ph/0311325](#)].
- [25] M. Ciafaloni, D. Colferai, G. P. Salam and A. M. Stasto, *Renormalization group improved small  $x$  Green's function*, Phys. Rev. D **68** (2003) 114003, [[hep-ph/0307188](#)].
- [26] M. Ciafaloni, D. Colferai, G. P. Salam and A. M. Stasto, *A Matrix formulation for small- $x$  singlet evolution*, JHEP **08** (2007) 046, [[0707.1453](#)].

[27] W. Li and A. M. Stasto, *Structure functions from renormalization group improved small  $x$  evolution*, *Eur. Phys. J. C* **82** (2022) 562, [2201.10579].

[28] L. V. Gribov, E. M. Levin and M. G. Ryskin, *Semihard Processes in QCD*, *Phys. Rept.* **100** (1983) 1–150.

[29] A. H. Mueller and J.-w. Qiu, *Gluon Recombination and Shadowing at Small Values of  $x$* , *Nucl. Phys. B* **268** (1986) 427–452.

[30] L. D. McLerran and R. Venugopalan, *Gluon distribution functions for very large nuclei at small transverse momentum*, *Phys. Rev. D* **49** (1994) 3352–3355, [hep-ph/9311205].

[31] L. D. McLerran and R. Venugopalan, *Computing quark and gluon distribution functions for very large nuclei*, *Phys. Rev. D* **49** (1994) 2233–2241, [hep-ph/9309289].

[32] L. D. McLerran and R. Venugopalan, *Green's functions in the color field of a large nucleus*, *Phys. Rev. D* **50** (1994) 2225–2233, [hep-ph/9402335].

[33] J. Jalilian-Marian, A. Kovner, L. D. McLerran and H. Weigert, *The Intrinsic glue distribution at very small  $x$* , *Phys. Rev. D* **55** (1997) 5414–5428, [hep-ph/9606337].

[34] J. Jalilian-Marian, A. Kovner and H. Weigert, *The Wilson renormalization group for low  $x$  physics: Gluon evolution at finite parton density*, *Phys. Rev. D* **59** (1998) 014015, [hep-ph/9709432].

[35] J. Jalilian-Marian, A. Kovner, A. Leonidov and H. Weigert, *The Wilson renormalization group for low  $x$  physics: Towards the high density regime*, *Phys. Rev. D* **59** (1998) 014014, [hep-ph/9706377].

[36] J. Jalilian-Marian, A. Kovner, A. Leonidov and H. Weigert, *The BFKL equation from the Wilson renormalization group*, *Nucl. Phys. B* **504** (1997) 415–431, [hep-ph/9701284].

[37] E. Iancu, A. Leonidov and L. D. McLerran, *Nonlinear gluon evolution in the color glass condensate. 1.*, *Nucl. Phys. A* **692** (2001) 583–645, [hep-ph/0011241].

[38] E. Iancu, A. Leonidov and L. D. McLerran, *The Renormalization group equation for the color glass condensate*, *Phys. Lett. B* **510** (2001) 133–144, [hep-ph/0102009].

[39] I. Balitsky, *Operator expansion for high-energy scattering*, *Nucl. Phys. B* **463** (1996) 99–160, [hep-ph/9509348].

[40] I. Balitsky, *Factorization and high-energy effective action*, *Phys. Rev. D* **60** (1999) 014020, [hep-ph/9812311].

[41] Y. V. Kovchegov, *Unitarization of the BFKL pomeron on a nucleus*, *Phys. Rev. D* **61** (2000) 074018, [hep-ph/9905214].

[42] Y. V. Kovchegov, *Small  $x$   $F_2$  structure function of a nucleus including multiple pomeron exchanges*, *Phys. Rev. D* **60** (1999) 034008, [[hep-ph/9901281](#)].

[43] Y. V. Kovchegov, J. Kuokkanen, K. Rummukainen and H. Weigert, *Subleading- $N(c)$  corrections in non-linear small- $x$  evolution*, *Nucl. Phys. A* **823** (2009) 47–82, [[0812.3238](#)].

[44] I. Balitsky and G. A. Chirilli, *Next-to-leading order evolution of color dipoles*, *Phys. Rev. D* **77** (2008) 014019, [[0710.4330](#)].

[45] T. Lappi and H. Mäntysaari, *Direct numerical solution of the coordinate space Balitsky-Kovchegov equation at next to leading order*, *Phys. Rev. D* **91** (2015) 074016, [[1502.02400](#)].

[46] J. Bartels and M. Wusthoff, *The Triple Regge limit of diffractive dissociation in deep inelastic scattering*, *Z. Phys. C* **66** (1995) 157–180.

[47] N. N. Nikolaev and W. Schafer, *Quenching of Leading Jets and Particles: The  $p_{\perp}$  Dependent Landau-Pomeranchuk-Migdal effect from Nonlinear  $k_{\perp}$  Factorization*, *Phys. Rev. D* **74** (2006) 014023, [[hep-ph/0604117](#)].

[48] K. Kutak and S. Sapeta, *Gluon saturation in dijet production in  $p$ -Pb collisions at Large Hadron Collider*, *Phys. Rev. D* **86** (2012) 094043, [[1205.5035](#)].

[49] A. van Hameren, P. Kotko, K. Kutak and S. Sapeta, *Small- $x$  dynamics in forward-central dijet decorrelations at the LHC*, *Phys. Lett. B* **737** (2014) 335–340, [[1404.6204](#)].

[50] A. van Hameren, P. Kotko, K. Kutak, C. Marquet, E. Petreska and S. Sapeta, *Forward di-jet production in  $p$ +Pb collisions in the small- $x$  improved TMD factorization framework*, *JHEP* **12** (2016) 034, [[1607.03121](#)].

[51] J. L. Albacete, G. Giacalone, C. Marquet and M. Matas, *Forward dihadron back-to-back correlations in  $p$ A collisions*, *Phys. Rev. D* **99** (2019) 014002, [[1805.05711](#)].

[52] A. Bhattacharya, R. Enberg, Y. S. Jeong, C. S. Kim, M. H. Reno, I. Sarcevic et al., *Prompt atmospheric neutrino fluxes: perturbative QCD models and nuclear effects*, *JHEP* **11** (2016) 167, [[1607.00193](#)].

[53] A. van Hameren, H. Kakkad, P. Kotko, K. Kutak and S. Sapeta, *Searching for saturation in forward dijet production at the LHC*, *Eur. Phys. J. C* **83** (2023) 947, [[2306.17513](#)].

[54] J. Berger and A. M. Stasto, *Small  $x$  nonlinear evolution with impact parameter and the structure function data*, *Phys. Rev. D* **84** (2011) 094022, [[1106.5740](#)].

[55] H. Mäntysaari and B. Schenke, *Confronting impact parameter dependent JIMWLK evolution with HERA data*, *Phys. Rev. D* **98** (2018) 034013, [[1806.06783](#)].

[56] J. L. Albacete, N. Armesto, J. G. Milhano, P. Quiroga-Arias and C. A. Salgado, *AAMQS: A non-linear QCD analysis of new HERA data at small- $x$  including heavy quarks*, *Eur. Phys. J. C* **71** (2011) 1705, [[1012.4408](#)].

[57] J. Cepila, J. G. Contreras and M. Matas, *Collinearly improved kernel suppresses Coulomb tails in the impact-parameter dependent Balitsky-Kovchegov evolution*, *Phys. Rev. D* **99** (2019) 051502, [[1812.02548](#)].

[58] E. Iancu, J. D. Madrigal, A. H. Mueller, G. Soyez and D. N. Triantafyllopoulos, *Collinearly-improved BK evolution meets the HERA data*, *Phys. Lett. B* **750** (2015) 643–652, [[1507.03651](#)].

[59] K. J. Golec-Biernat and M. Wusthoff, *Saturation effects in deep inelastic scattering at low  $Q^{**2}$  and its implications on diffraction*, *Phys. Rev. D* **59** (1998) 014017, [[hep-ph/9807513](#)].

[60] H1, ZEUS collaboration, H. Abramowicz et al., *Combination of measurements of inclusive deep inelastic  $e^\pm p$  scattering cross sections and QCD analysis of HERA data*, *Eur. Phys. J. C* **75** (2015) 580, [[1506.06042](#)].

[61] J. Bartels and K. Kutak, *A Momentum Space Analysis of the Triple Pomeron Vertex in pQCD*, *Eur. Phys. J. C* **53** (2008) 533–548, [[0710.3060](#)].

[62] D. V. Shirkov and I. L. Solovtsov, *Analytic model for the QCD running coupling with universal alpha-s (0) value*, *Phys. Rev. Lett.* **79** (1997) 1209–1212, [[hep-ph/9704333](#)].

[63] A. V. Kotikov, A. V. Lipatov, B. G. Shaikhatdenov and P. Zhang, *Transverse momentum dependent parton densities in a proton from the generalized DAS approach*, *JHEP* **02** (2020) 028, [[1911.01445](#)].

[64] H.-L. Lai, M. Guzzi, J. Huston, Z. Li, P. M. Nadolsky, J. Pumplin et al., *New parton distributions for collider physics*, *Phys. Rev. D* **82** (2010) 074024, [[1007.2241](#)].

[65] A. V. Kotikov and B. G. Shaikhatdenov,  *$Q^2$  evolution of parton distributions at small values of  $x$ : Effective scale for combined H1 and ZEUS data on the structure function  $F_2$* , *Phys. Atom. Nucl.* **78** (2015) 525–527, [[1402.4349](#)].

[66] L. Motyka and N. Timneanu, *Unintegrated gluon in the photon and heavy quark production*, *Eur. Phys. J. C* **27** (2003) 73–85, [[hep-ph/0209029](#)].

[67] G. A. Chirilli and Y. V. Kovchegov, *Solution of the NLO BFKL Equation and a Strategy for Solving the All-Order BFKL Equation*, *JHEP* **06** (2013) 055, [[1305.1924](#)].

[68] G. Beuf, *Improving the kinematics for low- $x$  QCD evolution equations in coordinate space*, *Phys. Rev. D* **89** (2014) 074039, [[1401.0313](#)].

[69] P. Caecal, F. Salazar, B. Schenke, T. Stebel and R. Venugopalan, *Back-to-Back Inclusive Dijets in Deep Inelastic Scattering at Small  $x$ : Complete NLO Results and Predictions*, *Phys. Rev. Lett.* **132** (2024) 081902, [2308.00022].

[70] K. Golec-Biernat and A. M. Stasto,  *$F_L$  proton structure function from the unified DGLAP/BFKL approach*, *Phys. Rev. D* **80** (2009) 014006, [0905.1321].

[71] J. C. Collins and R. K. Ellis, *Heavy quark production in very high-energy hadron collisions*, *Nucl. Phys. B* **360** (1991) 3–30.

[72] A. J. Askew, J. Kwiecinski, A. D. Martin and P. J. Sutton, *QCD predictions for deep inelastic structure functions at HERA*, *Phys. Rev. D* **47** (1993) 3775–3782.

[73] A. Bialas, H. Navelet and R. B. Peschanski, *QCD dipole model and  $k_T$  factorization*, *Nucl. Phys. B* **593** (2001) 438–450, [hep-ph/0009248].

[74] A. Bialas, H. Navelet and R. B. Peschanski, *Virtual photon impact factors with exact gluon kinematics*, *Nucl. Phys. B* **603** (2001) 218–230, [hep-ph/0101179].

[75] D. Colferai, W. Li and A. M. Stasto, *Renormalization group improved photon impact factors and the high energy virtual photon scattering*, *JHEP* **01** (2024) 106, [2311.07443].

[76] G. Beuf, H. Hänninen, T. Lappi and H. Mäntysaari, *Color Glass Condensate at next-to-leading order meets HERA data*, *Phys. Rev. D* **102** (2020) 074028, [2007.01645].

[77] A. J. Askew, J. Kwiecinski, A. D. Martin and P. J. Sutton, *Properties of the BFKL equation and structure function predictions for HERA*, *Phys. Rev. D* **49** (1994) 4402–4414, [hep-ph/9310261].

[78] A. Donnachie and P. V. Landshoff, *Total cross-sections*, *Phys. Lett. B* **296** (1992) 227–232, [hep-ph/9209205].

[79] K. Watanabe, B.-W. Xiao, F. Yuan and D. Zaslavsky, *Implementing the exact kinematical constraint in the saturation formalism*, *Phys. Rev. D* **92** (2015) 034026, [1505.05183].

[80] J. L. Albacete, *Resummation of double collinear logs in BK evolution versus HERA data*, *Nucl. Phys. A* **957** (2017) 71–84, [1507.07120].

[81] J. Kwiecinski, A. D. Martin and P. J. Sutton, *Constraints on gluon evolution at small  $x$* , *Z. Phys. C* **71** (1996) 585–594, [hep-ph/9602320].

[82] C. Marquet, *Forward inclusive dijet production and azimuthal correlations in  $p(A)$  collisions*, *Nucl. Phys. A* **796** (2007) 41–60, [0708.0231].

[83] J. L. Albacete and C. Marquet, *Gluon saturation and initial conditions for relativistic heavy ion collisions*, *Prog. Part. Nucl. Phys.* **76** (2014) 1–42, [1401.4866].

- [84] M. Deak, F. Hautmann, H. Jung and K. Kutak, *Forward Jet Production at the Large Hadron Collider*, *JHEP* **09** (2009) 121, [0908.0538].
- [85] M. Deak, F. Hautmann, H. Jung and K. Kutak, *Forward-Central Jet Correlations at the Large Hadron Collider*, 1012.6037.